Using MESA to Compute Statistical Distributions of IMF Model Parameters

Curran D. Muhlberger

Department of Physics,
Cornell University,
Ithaca, New York 14853,
USA

We develop techniques to probe the relative likelihoods of IMF models given an observed H-R diagram from a region of extended continuous starbirth. Our methods are informed by the results of stellar evolution simulations performed with the new MESA code. Using sample data from Hipparcos, we compute the statistical distribution of exponents for power law models of the IMF. Though unconsidered systematic effects dominate the analysis, voiding any physical significance of these sample results, our implementation succeeds in computing exact probabilities for observational data sets given any model IMF and can easily be used to compare the likelihoods of models from different families.

I. INTRODUCTION

In 1954, E. Salpeter used the observed luminosity function for stars on the main sequence to infer the rate of star formation as a function of mass, assuming that stars of a given mass were born at a constant rate over the past $5\,\mathrm{Gyr}$ (Salpeter, 1955). He called this rate the "original mass function," and noted that a power law form fitted the contemporary data quite well. Now known as the initial mass function (IMF), this birth rate so far appears to be relatively universal. It is often modeled by a piecewise power law whose behavior above $0.5M_\odot$ remains consistent with Salpeter's original exponent of $\Gamma = -1.35$ (Kroupa, 2001).

While Salpeter's work considered a luminosity function $\phi(m)$ for main-sequence stars, today we can use stellar evolution simulations to consider data on the entire H-R diagram. The goal of this study is to compute the probability of observing any observed H-R diagram (defined as a collection of temperature-luminosity pairs) given a particular IMF. To perform the necessary simulations, we use the Modules for Experiments in Stellar Astrophysics (MESA) open-source software library (Paxton *et al.*, 2010).

II. PROBABILITY THEORY

Our goal is to compute probability ratios for various models of the IMF given a set of observational data. With the ability to compute such ratios, we can specialize to a particular family of models and explore the statistical distribution of their parameters. Using Bayes's theorem, denoting a pair of models as H_1 and H_2, we find that

$$\frac{P(H_1|\text{data})}{P(H_2|\text{data})} = \frac{P(\text{data}|H_1)}{P(\text{data}|H_2)} \times \frac{P(H_1)}{P(H_2)} \times \frac{P(\text{data})}{P(\text{data})}.$$

In this study, we do not consider any *a priori* preference for one of the models. Applying the principle of indifference, we adopt a uniform prior for $P(H_1)$ and $P(H_2)$, reducing the above to simply

$$\frac{P(H_1|\text{data})}{P(H_2|\text{data})} = \frac{P(\text{data}|H_1)}{P(\text{data}|H_2)}.$$

If we wish to process data from another star forming region in the future, on the other hand, then the probability ratios resulting from the first data set can be used as priors when analyzing the second:

$$\frac{P(H_1|\text{data}_2)}{P(H_2|\text{data}_2)} = \frac{P(\text{data}_2|H_1)}{P(\text{data}_2|H_2)} \times \frac{P(H_1|\text{data}_1)}{P(H_2|\text{data}_1)}.$$

Specializing this formula to the problem at hand, our data is in the form of color and luminosity observations $\{T_i, L_i\}$, where

$$P(T_i, L_i) = P(\log(T_{\text{eff}}/\text{K}) = T_i \cap \log(L/L_\odot) = L_i).$$

If $\xi(m)$ is the IMF associated with a model H, giving the relative birth rates of stars of mass m, then denote

$$P(m_1, m_2|H) = \frac{\int_{m_1}^{m_2} \xi(m)\,d(\log m)}{\int_{m_{\min}}^{m_{\max}} \xi(m)\,d(\log m)}.$$

Note that the IMF $\xi(m)$ is defined by

$$dN = \xi(m)d(\log m)\frac{dt}{T_0},$$

where N is the number of stars born per unit volume in the time interval dt. Salpeter (Salpeter, 1955) proposed a power law of the form

$$\xi(m) \propto m^\Gamma,$$

which can be normalized for any mass range $[m_1, m_2]$ by noting that

$$\int_{m_1}^{m_2} m^\Gamma d(\log m) = \int_{\log(m_1)}^{\log(m_2)} 10^{\Gamma x} dx$$
$$= \frac{10^{\Gamma\log(m_2)} - 10^{\Gamma\log(m_1)}}{\Gamma\ln(10)}.$$

Since we perform a finite number N^* of stellar evolutions, each characterized by a zero-age main sequence (ZAMS) mass m_i, it is natural to compute probability densities for observations given that observed star has a mass $m \in [m_i, m_{i+1}]$. Then the total probability density of that observation, given a particular IMF, is

$$P(T, L|H) = \sum_{i=1}^{N^*-1} P(T, L|m_i, m_{i+1}|H)P(m_i, m_{i+1}|H).$$

If stars have been continuously related at the same rate for some time t, then the quantity $P(T, L|m_i, m_{i+1}|H)$ is proportional to the amount of time a stellar evolution curve of age $< t$ spends in the vicinity of (T, L), integrated over all ZAMS masses between m_1 and m_2. Computing it from MESA simulations is described in detail in Section IV.

Now, rather than a single observation, we have a set of N^{obs} observations, and we want to know the probability of

observing that particular set among all possible sets of the same size. To do this, we divide the observation space $\{T, L\}$ into N^{hist} histogram bins, then count the number of data points (T_i, L_i) occurring in each bin. The likelihood of observing a particular number of points in each bin is given by a binomial distribution with p equal to the integral of $P(T, L|H)$ over the bin. To compute the probability of observing the collection as a whole, we iteratively use the conditional probability relation

$$P(A \cap B) = P(A|B)P(B),$$

where A is the event of finding the observed number of particles in a particular bin, and B is the set of observations in all previously-processed bins. In order to compute $P(A|B)$, we process the bins sequentially and keep track of the total number of observations processed (n) and the total probability represented by those bins (Σp). Then, the conditional probability of observing k points in bin i is

$$P(k \text{ in bin } i | n \text{ in bins } 0 \ldots i-1) = \binom{N^{\text{obs}} - n}{k} \left(\frac{p_i}{1 - \Sigma p} \right)^k \left(1 - \frac{p_i}{1 - \Sigma p} \right)^{N^{\text{obs}} - n - k}.$$

The product of these probabilities is the likelihood of observing this particular collection of observations among all possible histograms of N^{obs} points. That is, we have computed

$$P(\{T_i, L_i\}|H) = \prod_{i=1}^{N^{\text{hist}}} \binom{N^{\text{obs}} - \sum_{j<i} n_j}{n_i} \left(\frac{p_i}{1 - \sum_{j<i} p_j} \right)^{n_i} \left(1 - \frac{p_i}{1 - \sum_{j<i} p_j} \right)^{N^{\text{obs}} - \sum_{j \leq i} n_j}.$$

We can now measure the relative probabilities of any two models for the IMF.

III. STELLAR EVOLUTION

In order to compute $P(T, L|m_1, m_2|H)$ as required by the above formula, we need to know how long stars of masses m_i live in various regions of the H-R diagram. To do this, we employ the stellar evolution code *MESA star*, which computes a sequence of stellar models in hydrostatic equilibrium while incorporating a wide array of microphysical and macrophysical effects. Given an ZAMS mass m, we evolve the star from its pre-main sequence collapse until it lands on the asymptotic giant branch (AGB) or becomes a white dwarf.

Our simulations incorporate an extended nuclear reaction network (denoted `h_he` in MESA) providing nearly complete coverage of hydrogen and helium burning processes. It includes the following isotopes: ^{1}H, ^{2}H, ^{3}He, ^{4}He, ^{7}Li, ^{7}Be, ^{8}B, ^{12}C, ^{13}C, ^{13}N, ^{14}N, ^{15}N, ^{14}O, ^{15}O, ^{16}O, ^{17}O, ^{18}O, ^{17}F, ^{18}F, ^{19}F, ^{18}Ne, ^{19}Ne, ^{20}Ne, ^{22}Ne, ^{22}Mg, and ^{24}Mg. Above $6 - 8M_\odot$ these may not be sufficient, and other networks are available to better model C/O burning and α chains. However, due to time constraints, all models in this study used the above

H/He network. As the vast majority of a star's life is spent on the main sequence, the neglected physics in advanced stages of evolution should not have a large impact on the probability distribution we construct from the data.

Other simulation parameters include opacity tables from Grevesse and Sauval (Grevesse and Sauval, 1998), RGB mass loss based on a 1975 wind scheme from D. Reimers, and AGB mass loss based on a 1995 wind scheme from T. Blocker. The atmosphere is treated by integrating the equation of hydrostatic balance using the Krishna Swamy $T - \tau$ relation from $\tau = 10^{-5}$ to $\tau = 0.312$ (Krishna Swamy, 1966).

We halt the evolution upon the first AGB thermal pulse, which is detected by the presence of a helium-burning convective zone after central helium has been depleted. Low-mass stars will never reach this situation, so their evolution is stopped when the plasma interaction parameter Γ exceeds 25, which occurs during the white dwarf cooling phase, or when the simulation process hangs.

We performed 36 stellar evolution simulations with $\log(m/M_\odot)$ evenly distributed between -0.5 and 1.5. These simulations were performed on the computing cluster *Zwicky* at Caltech, with each process using three OpenMP threads.

To prepare the simulation output for analysis and plotting,

we removed some unwanted features from the evolution tracks. These include model searches leading up to the pre main sequence collapse, which are identified as all models prior to the last early minimum in hydrogen burning luminosity. Additionally, some low-mass models went on large excursions in the H-R diagram during the white dwarf cooling phase. As we do not expect to include white dwarfs in the observational data at this stage, and as these excursions would break assumptions in data processing algorithm described in Section IV, they were removed as well. Similarly, spirrious features during advanced stages of high-mass evolution were removed, as the chosen nuclear reaction network was not sufficient to model the physics in these regimes. Finally, sharp features common to simulations of similar masses were manually tagged to allow the models to be parameterized by a single time-like variable.

The evolutionary tracks of all 36 simulations are plotted in Figure 1 and are in visual agreement with similar tracks published in the MESA instrument paper (Paxton *et al.*, 2010).

IV. DATA PROCESSING

Given a pair of stellar evolutions with ZAMS masses m_1 and M_2, it is a far from trivial task to compute $P(T, L | m_1, m_2 | H)$. We take the following approach, which requires that the evolutionary tracks on the H-R diagram be reasonably similar in shape. First, we require a parameter for each curve that increases monotonically with stellar age and is equal at corresponding points on neighboring curves. We choose a scaling of the stellar age such that up to two distinguished features of neighboring tracks are brought into alignment. Given the low order of accuracy of our methods at this time, the choice of this parameter can have a significant impact on the resulting probability distributions when only a small number of simulations are available.

Given such a parameter, we can now construct bridges between the two tracks, thus dividing the space between the two curves into a set of (possibly overlapping) quadrilaterals. Linear interpolation along the tracks is used when no data point exists at a desired parameter value. The probability of being found in a particular quadrilateral is equal to the average of the time spent on each of the two bounding track segments divided by the age of the star forming region we are considering. The lack of interpolation at this point in the scheme represents a potentially significant loss of accuracy, so we compensate by running many evolutions and recording data at high temporal resolutions along their tracks. The probability density in this region is then equal to this probability divided by the area of the quadrilateral. If multiple regions overlap, then the probability density in the overlapped region is equal to the sum of the individual densities.

To compute probabilities over histogram bins, we need to integrate this resulting density over each histogram bin. To do this, we compute the area of intersection of each quadrilateral with each histogram bin and multiply that quadrilateral's prob-

ability density by this area. The region of overlap is found by intersecting the quadrilateral's perimeter with the histogram grid and then discarding all points outside the bin. Areas of N-gons are computed using the formula

$$A = \frac{1}{2} \left| \sum_{i=0}^{N-1} x_i y_{i+1} - x_{i+1} y_i \right|$$

(where indices are taken modulo N), as described in Numerical Recipes's chapter on computational geometry (Press *et al.*, 2007).

By summing the histograms for each mass range weighted by the integrated IMF, we can compute the probability of observing a star in any bin relative to any other. This probability distribution is plotted for the case of Salpeter's $\Gamma = -1.35$ IMF in Figure 2. If we sum the probabilities in each bin, we find that roughly only 85% is accounted for. The remaining 15% represents high-mass stars with pre-AGB lifetimes shorter than the age of our region (here, 5 Gyr), which cannot be observed as stars (we assume that our data is free of supernova remnants). A proper analysis of observational data, then, would require an estimate of the number of unobserved stars, though for the purposes of this introductory study, we neglect this correction below.

V. OBSERVATIONS

Now that we have a model-dependent theoretical distribution for the properties of stars in an active star-forming region, we can ask how well real observations agree with the distribution implied by any given model. A thorough analysis of such data is beyond the scope of this work, but we can nevertheless demonstrate our methods with an example dataset. For this purpose, we query data from the 1997 Hipparcos and Tycho catalogs (Perryman and ESA, 1997) using *VizieR*, selecting all 2612 stars within 1000 arcseconds of the Orion Nebula Cluster (ONC).

The observations consist of the apparent magnitude in the Johnson V band, the trigonometric parallax, and the Johnson $B - V$ colour. To compare these with our theory, we must convert them to effective temperature and bolometric luminosity. The relationship between T_{eff} and $B - V$ has been modeled by P. Flower using a 7th-degree polynomial (Flower, 1996) whose coefficients were reprinted with corrections and higher precision by Torres (Torres, 2010).

Converting the apparent magnitude to a luminosity is slightly more involved. First we compute a temperature-dependent bolometric correction factor BC to convert the V-band apparent magnitude to a bolometric one. The correction factor was also modeled by Flower, this time as a piecewise 5th-order polynomial, and reprinted correctly by Torres. Next, we find the absolute magnitude using the parallax. If p is the parallax angle in milliarcseconds, then

$$M = V + BC + 5\log(p) - 10.$$
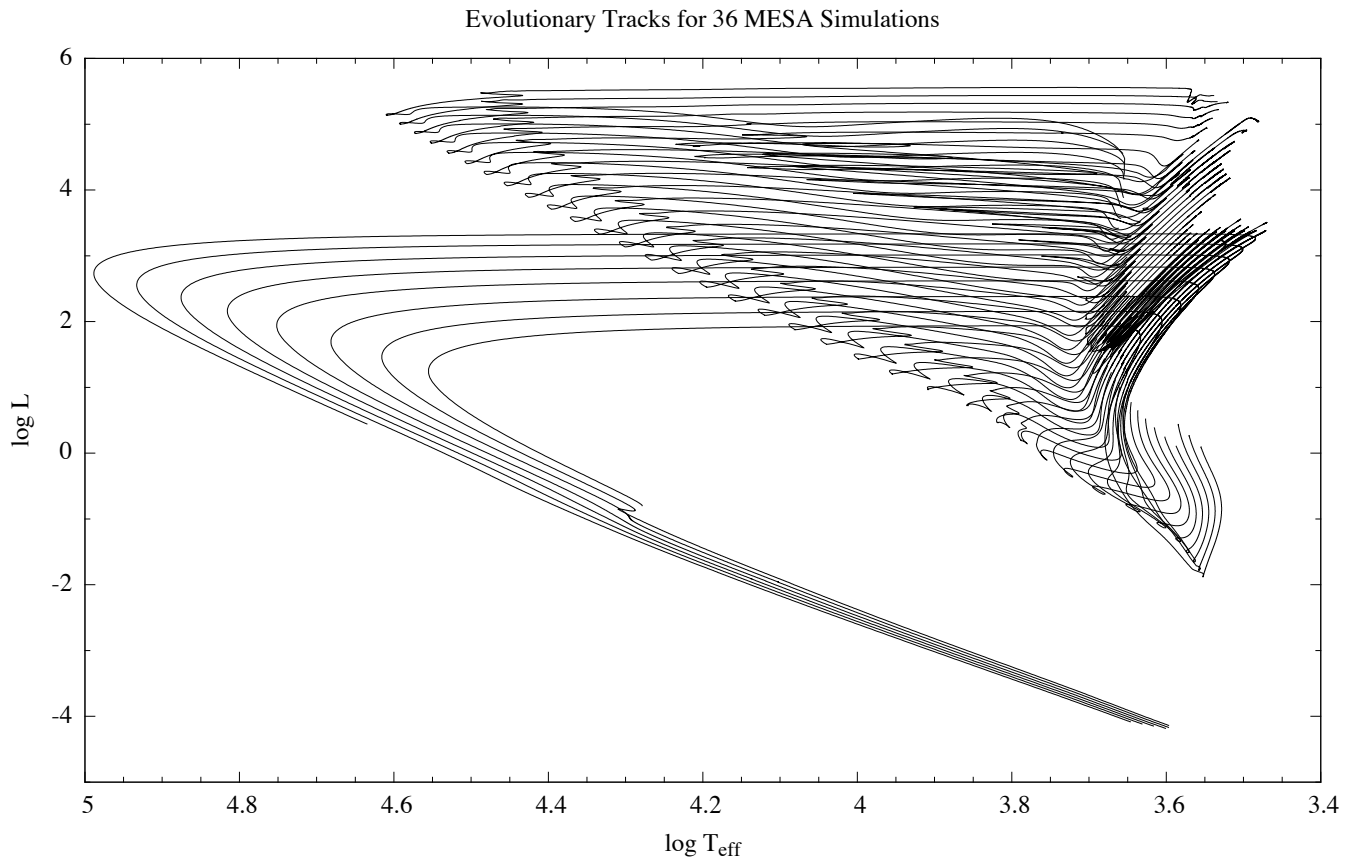
Evolutionary Tracks for 36 MESA Simulations

Figure 1 Simulated evolution tracks for 36 stars with masses $0.3 - 30 M_\odot$. Tracks begin during pre-main sequence collapse and continue until the star either experiences an AGB thermal pulse or cools off as a white dwarf.

Finally, we convert to solar luminosities, using the value $M_{bol,\odot} = 4.73$ as specified by Torres for use with Flower's formulas (Torres, 2010):

$$\log(L/L_\odot) = -0.4(V + BC + 5\log(p) - 14.73).$$

The resulting H-R diagram is shown in Figure 3.

To determine the likelihood of this dataset, we sort it into histogram bins and use the binomial distribution to compute the probability of finding the observed number of counts in each bin, given the observations in previous bins.

When processing the observational data, the GNU Scientific Library (Galassi *et al.*, 2003) was used to evaluate Flower's fitting polynomials and the binomial distribution for each bin.

VI. ANALYSIS AND RESULTS

Unfortunately, when processing the entire dataset, even using only 64 histogram bins, the log probabilities involved quickly underflow, making this problem awkward to treat numerically (though arbitrary precision arithmetic could be considered for future studies). As a workaround, we limit ourselves to a subset of 500 observations from the original

sample dataset. Now, assuming an age of 5 Gyr, the average age of stars in the galactic field (Kroupa, 2001), we can compute the exact probability of observing this binned data given a candidate IMF.

Limiting ourselves to power laws, we scan over the power law index Γ and produce the plot shown in Figure 4. The model peaks at about $\Gamma = -0.14$ and strongly disfavors Salpeter's 1955 value of -1.35. As discussed in Section II, the relative probability of a particular power law exponent being correct compared to another is 10 to the power of the difference in their respective log probabilities. In this instance, given the data, a $\Gamma = -0.14$ model is about 10^{170} times more likely than a $\Gamma = -1.35$ model.

This result is merely an example of the method in practice, and we mean it to imply no physical significance. A proper analysis of observational data would require correcting for a large number of systematic effects, including:

- Ensuring that all observed stars come from the same star-forming region

- Accounting for detector bias in counts of dim stars
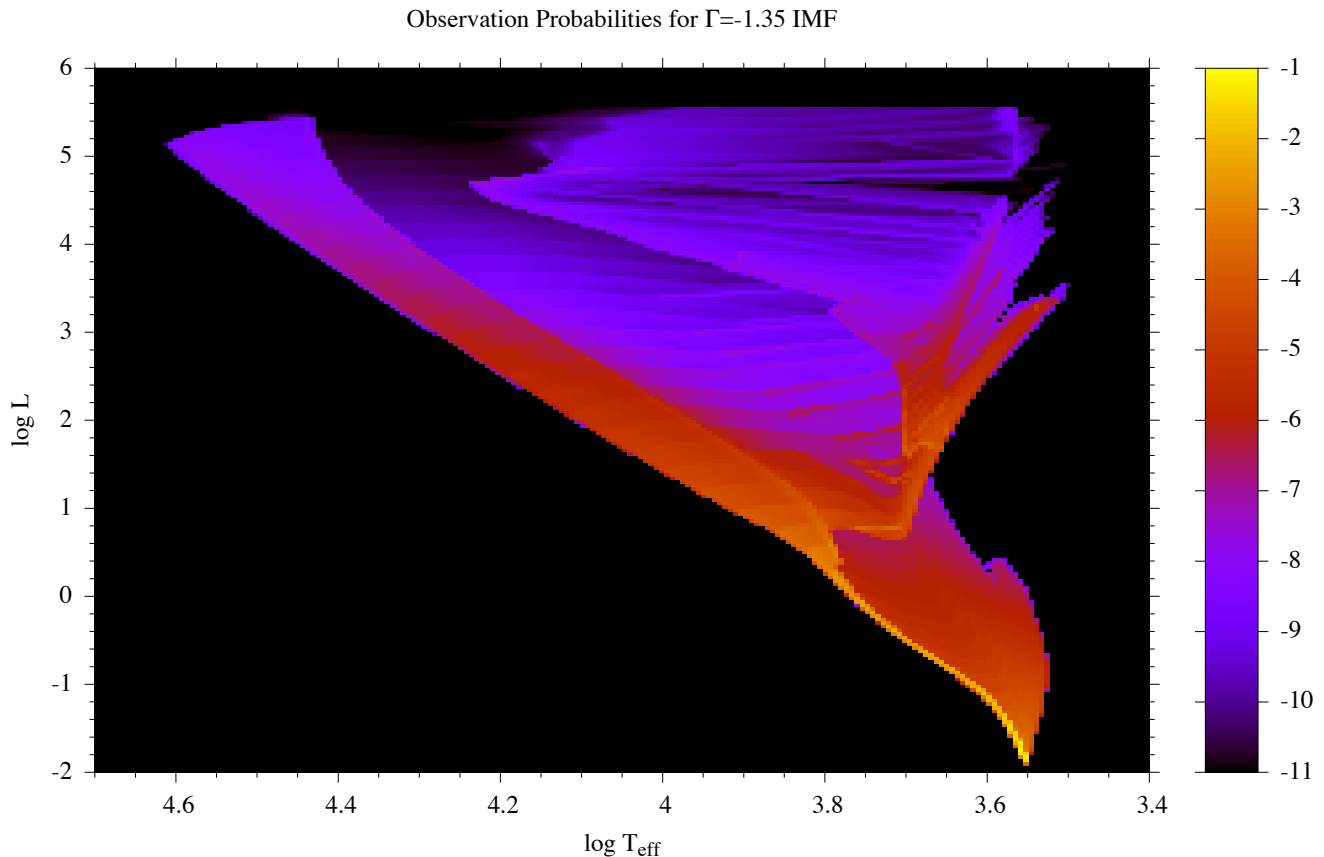
- Avoiding unresolved binaries

Figure 2 Log probability of observing a star in various regions of the H-R diagram for a $\Gamma = -1.35$ power law IMF and an age of 5.0 Gyr.

- Checking the accuracy of temperature and luminosity conversions

Additionally, we would want to scan over the proposed age of the region as well, producing a 2-dimensional relative probability distribution. Many of these issues are the same as those mentioned by P. Kroupa regarding measuring variations in the IMF (Kroupa, 2001), but our method notably accounts for issue (iva) in his paper by utilizing full stellar evolution tracks from MESA.

Regarding this sample dataset, there is a significant lack of low-mass stars visible in Figure 3, which will bias the results in favor of less negative values of Γ – exactly what we find here.

VII. CONCLUSIONS

Due to these unconsidered systematic effects in the sample data chosen, this study probes no new physics on its own, but it does result in a framework for conducting rigorous tests of models of the IMF using color, brightness, and distance observations not limited to the main sequence.

The idea of computing the exact probability of observing a collection of temperatures and luminosities, independent of

the order in which measurements were taken, is an appealing prospect that does not turn out to be practical for even moderately large datasets. As the number of histogram bins increases, the number of possible frequency matrices for a fixed number of observations increases extremely rapidly, and the probabilities quickly underflow. While this method does produce exact probabilities for a small number of observations and a coarse binning, this statistic is probably less useful than a simple p-value.

On the other hand, when available, these exact probabilities do lead to exact probability ratios when comparing two models, thus allowing us to say that a $\Gamma = -0.15$ model is 10^{170} times more likely than Salpeter's original $\Gamma = -1.35$ model given this dataset. Systematic errors obviously dominate this example analysis, but the procedure is nevertheless sound.

What we have shown, then, is that modern stellar evolution codes like MESA can be used to perform batches of simulations that allow for a more complete analysis of models of the IMF. Future work can potentially use these techniques to perform multi-parameter fits to the IMF in various star-forming regions to further the search for systematic variations.
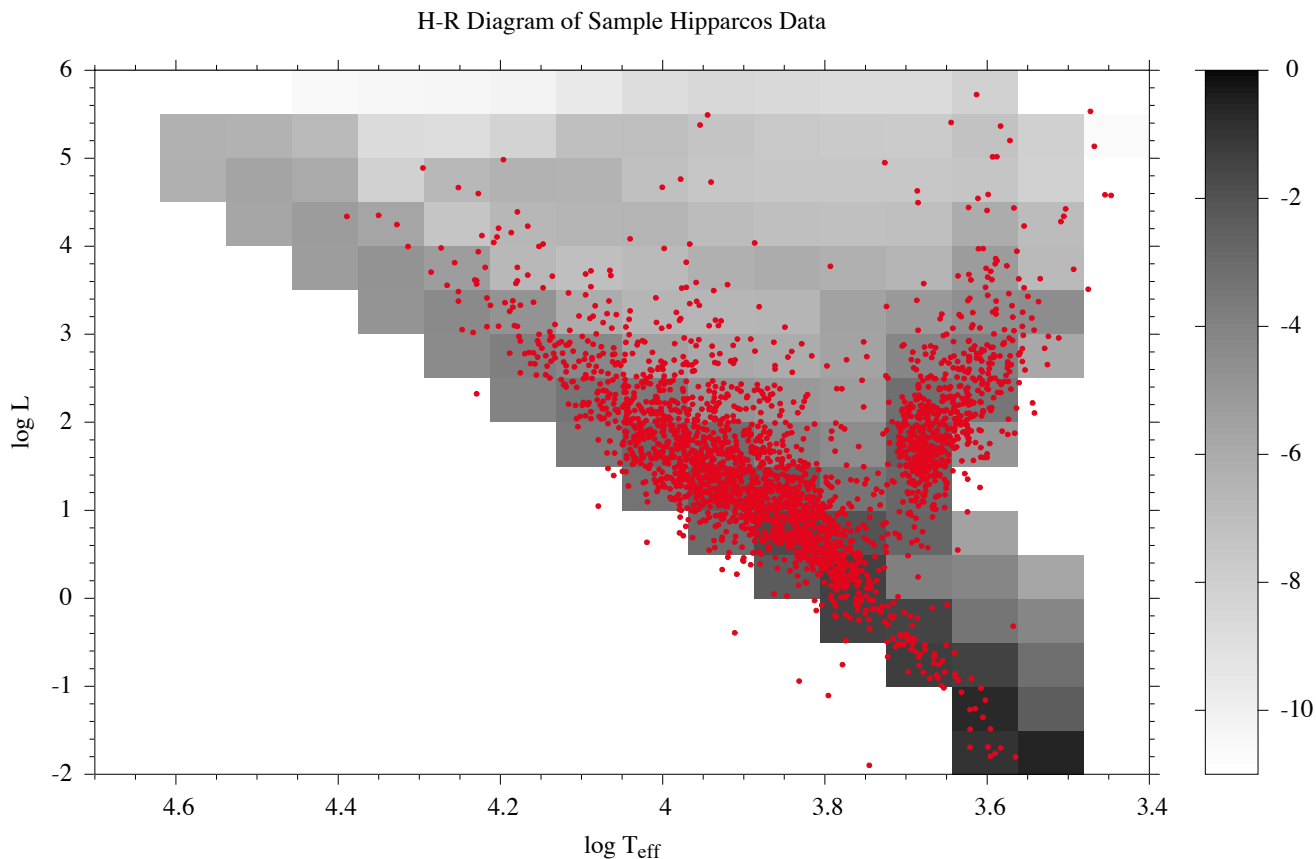
H-R Diagram of Sample Hipparcos Data

Figure 3 Plot of about 2600 Hipparcos observations within 1000 arcmin of ONC, overlaying a coarse binning of the probability distribution implied by a $\Gamma = -1.35$ power law IMF with an age of 5.0 Gyr.
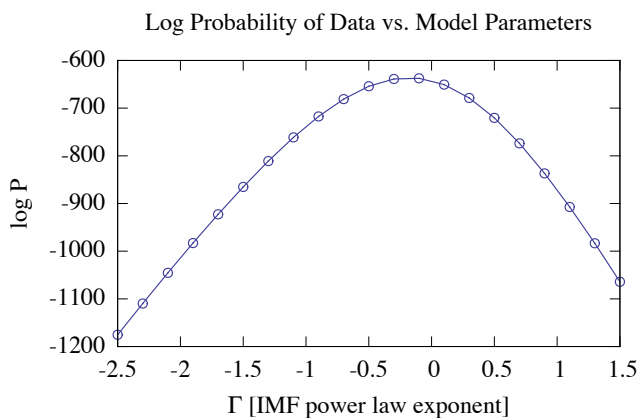
Log Probability of Data vs. Model Parameters

Figure 4 Probability of observing the sample dataset for various values of the IMF power law exponent $\Gamma = -1.35$, assuming an age of 5.0 Gyr. The relative probability of any two values of Γ is 10 to the power of the difference between their ordinates.

REFERENCES

Flower, P. J. (1996), Astrophys. J. **469**, 355.

Galassi, M., J. Davies, J. Theiler, G. Gough, Brianand Jungman, M. Booth, and F. Rossi (2003), *Gnu Scientific Library: Reference Manual* (Network Theory Ltd.).

Grevesse, N., and A. Sauval (1998), Space Science Reviews **85**, 161, 10.1023/A:1005161325181.

Krishna Swamy, K. S. (1966), Astrophys. J. **145**, 174.

Kroupa, P. (2001), Mon. Not. R. Astron. Soc. **322**, 231.

Paxton, B., L. Bildsten, A. Dotter, F. Herwig, P. Lesaffre, and F. Timmes (2010), ArXiv e-prints arXiv:1009.1622 [astro-ph.SR].

Perryman, M. A. C., and ESA, Eds. (1997), *ESA Special Publication*, ESA Special Publication, Vol. 1200.

Press, W. H., S. A. Teukolsky, W. T. Vetterling, and B. P. Flannery (2007), *Numerical Recipes*, 3rd ed. (Cambridge University Press).

Salpeter, E. E. (1955), Astrophys. J. **121**, 161.

Torres, G. (2010), The Astronomical Journal **140** (5), 1158.